

Zeolitic imidazolate framework-67 nanocrystal for high concentration Cr(VI) adsorption: a self-sacrifice process

Shaojun Li, Xiaoxuan Fan, Zhongping Chen*, Lei Bai*

College of Chemistry and Materials Engineering, Anhui Science and Technology University, Bengbu, Anhui, 233030, China, emails: chenzp322@sohu.com (Z.P. Chen), baileiwj2014@163.com (L. Bai), lishjunleon@163.com (S.J. Li), fanxiaoxuan2000@163.com (X.X. Fan)

Received 19 May 2022; Accepted 21 September 2022

ABSTRACT

A nanosized zeolitic imidazolate framework-67 (ZIF-67) was employed for the adsorption of Cr(VI) under a neutral solution. It was discovered that the ZIF-67 demonstrated a high adsorption of Cr(VI) for the first ($43.1 \text{ mg}\cdot\text{g}^{-1}$) and second run ($40.2 \text{ mg}\cdot\text{g}^{-1}$). However, a self-sacrifice process of ZIF-67 was evidenced, possibly due to the oxidability of Cr(VI) and pH change, which resulted in a dramatic decrease of adsorption ability in the third run ($16.6 \text{ mg}\cdot\text{g}^{-1}$). The adsorption process and its kinetics fitted the Langmuir model and pseudo-second-order rate equation and a multiple adsorption process was suggested.

Keywords: Zeolitic imidazolate framework-67 (ZIF-67); Adsorption; Cr(VI) removal; Self-sacrifice process

1. Introduction

Zeolitic Imidazolate Frameworks (ZIFs) such as zeolitic imidazolate framework-67 (ZIF-67) synthesized by cobalt ions and 2-Methylimidazole is a kind of porous crystalline materials [1]. In addition of the synthesis of cobalt-based solids for energy and environmental catalysis, they are widely employed in the catalytic reactions and separation process due to the high stability, porosity and organic functional groups [2]. For example, as-mentioned ZIF-67 had been explored in the adsorption of various dye molecules based on the electrostatic interactions, coordination interactions and hydrogen bonding interactions [3,4]. On the other hand, as a noxious heavy metal ion, Cr(VI) ion has been confirmed to cause harmful effect on both human body and environment. It was discovered that unlike the other transition metal ions, the addition of inorganic base was not able to dispose it and the variation of pH could only change the form of Cr(VI) [5]. It was suggested that among lots of methods, the adsorption treatment was one of promising way to eliminate

the Cr(VI) from aqueous solution [6]. Thus, various materials, such as biosorbents and carbon-based adsorbents were developed to adsorb the Cr(VI) ion from aqueous solution based on the different mechanistic interactions [7]. It was worth mentioning that the ZIF-67 solid was also used to remove the Cr(VI) ions from the water via the electrostatic adsorption and ion-exchange and at low Cr(VI) concentration, the adsorption behavior of ZIF-67 was well investigated [8]. However, the mutual influence of ZIF-67 and high Cr(VI) concentration is less studied, for instance, the reusability and structure of ZIF-67 after adsorption.

In this work, a nano-sized ZIF-67 was synthesized by a hydrothermal method and used for high Cr(VI) adsorption ($80\text{--}180 \text{ mg}\cdot\text{L}^{-1}$). The results suggested that at a relatively high Cr(VI) concentration, the ZIF-67 could be reused for twice and an obvious decrease adsorption quantity was observed, possibly due to the heavily damaged structure as suggested by the investigation from X-ray diffraction and scanning electron microscope. Besides, a reduction-adsorption process was observed for the removal of Cr(VI) and

* Corresponding authors.

the detailed study suggested that the adsorption process and its kinetics fitted the Langmuir model and pseudo-second-order rate equation. The present work evidenced the application of metal organic framework such as ZIF-67 in the adsorption of metal ions with strong oxidability as well as highlighted the advantage and drawbacks of nano-sized ZIF-67 in the Cr(VI) treatment.

2. Experimental

2.1. Materials

Cobalt nitrate hexahydrate [$\text{Co}(\text{NO}_3)_2 \cdot 6\text{H}_2\text{O}$] and aqueous ammonia were analytical pure and purchased from Sinopharm Chemical Reagent Co., Ltd., China. 2-Methylimidazole was analytical pure and purchased from Aladdin Reagent Co., Ltd., China.

2.2. Synthesis of ZIF-67 nanocrystal

1 mmol $\text{Co}(\text{NO}_3)_2 \cdot 6\text{H}_2\text{O}$ was first dissolved in 5 mL distilled water, which was denoted as solution A. Then, 0.1 mL aqueous ammonia and 20 mmol 2-methylimidazole were dissolved in 5 mL distilled water to form solution B. The solution B was added into solution A under stirring and then the mixture was transformed into 30 mL Teflon-lined stainless-steel autoclave, which was treated at 393 K for 30 min before cooling to room temperature. The purple solid was obtained after washing by ethanol for 3 times by centrifugation and drying at 333 K overnight.

3. Characterization

X-ray diffraction (XRD) was performed on an XRD-6000 X-ray diffractometer (XRD, SHIMADZULIMITED Corp.) at a scanning rate of 20°/min from 5° to 55°. Field emission scanning electron microscope (FE-SEM) was performed on the Hitachi-S4800. X-ray photoelectron spectroscopy (XPS) was performed using a Thermo ESCALAB 250 instrument with a monochromatic Al K α ($h\nu = 1,486.6$ eV) X-ray source. Ultraviolet–visible (UV–Vis) absorption spectra were obtained on a Shimadzu UV-2600 spectrophotometer with a moderate scanning rate.

3.1. Adsorption experiments

Before the test, the as-obtained ZIF-67 was dried at 393 K for 2 h. Then, 50 mg ZIF-67 was added into 30 mL aqueous solution containing different amount of $\text{K}_2\text{Cr}_2\text{O}_7$ (80–180 $\text{mg}\cdot\text{L}^{-1}$). After well-dispersed by ultrasonication, 1 mL solution was draw at certain time, centrifuged and 0.2 mL of the clear solution was added into 4 mL acid solution containing 2 mL diphenylcarbazide, 1 mL H_2SO_4 and 1 mL H_3PO_4 . After 10 min, the solution was analyzed by Shimadzu UV-2600 UV-vis spectrophotometer.

The ZIF-67 after first, second and third run of Cr(VI) adsorption was named as S-1, S-2 and S-3, respectively.

4. Results

First of all, the adsorption performance of the nano-sized ZIF-67 crystal was investigated by removing Cr(VI)

in the distilled water. Fig. 1 shows the time profiles of the Cr(VI) removal with 80 $\text{mg}\cdot\text{L}^{-1}$ $\text{K}_2\text{Cr}_2\text{O}_7$ for three runs. It was suggested that with the increased of the time, the adsorption amount was increase and then turned very slowly. For the first and second run, it can be seen that the equilibrium adsorption capacities were 43.1 and 40.2 $\text{mg}\cdot\text{g}^{-1}$, respectively. However, for the third run, the equilibrium adsorption capacity was dramatically decreased to 16.6 $\text{mg}\cdot\text{g}^{-1}$ (Fig. S1 for the UV-Vis spectra). This observation confirmed that the present ZIF-67 displayed a high adsorption ability and on the other hand, the ZIF-67 could not be used after second run. Besides, Fig. 1B suggested that the adsorption capacity of Cr(VI) onto the ZIF-67 increased from 40.2 to 50.2 and 75.1 $\text{mg}\cdot\text{g}^{-1}$ with the increase of the initial concentration of Cr(VI) from 80 to 130 and 180 $\text{mg}\cdot\text{L}^{-1}$ (Fig. S2 for the UV-Vis spectra). This behavior could be attributed to the enhancement of the driving force with increasing initial concentration of Cr(VI). On the contrary, there is a decrease in the removal percentage of Cr(VI) with the increase in the initial Cr(VI) concentration which may be due to the insufficiency of the active sites that required for adsorption of high concentration of Cr(VI).

To understand the adsorption process, Langmuir and Freundlich adsorption models were applied to analyze the experimental data. Langmuir model suggested that the adsorbed molecules/ions were independent of and attached to the adsorbent surface in a single layer. While, the Freundlich model suggested that the adsorbent surface provided heterogeneous adsorption sites and the adsorbed molecules/ions had a mutual effect on each other. As shown in Fig. S3, the Langmuir model with a higher correlation coefficients (R^2 , 0.91) value than the Freundlich model (0.86) indicated that the adsorption process could be apt to monolayer adsorption [9]. Furthermore, the kinetic of Cr(VI) adsorption on the ZIF-67 nanocrystal were further investigated by using pseudo-second-order kinetic model. The kinetic parameters and the R^2 can be determined by linear regressions, which were estimated to be 0.999, 0.999 and 0.999 for the first, second and third run, respectively, as shown in Fig. 1C with 80 $\text{mg}\cdot\text{L}^{-1}$ $\text{K}_2\text{Cr}_2\text{O}_7$. The similar phenomena were also observed under different Cr(VI) concentration as displayed in Fig. 1D.

In order to illustrate the structure change, the fresh ZIF-67 and the solids after each adsorption test were investigated by XRD and the patterns were displayed in Fig. 2. The presence of the typical peaks at about 2θ value of 7.30°, 10.36°, 12.67° and 17.91° confirmed the formation of crystallized ZIF-67 [10]. After the first run of Cr(VI) adsorption, the main peaks remained with a decrease of the intensity, indicating that the ZIF-67 was almost kept. However, for the second and third run, we can see that the peaks corresponded to ZIF-67 totally disappeared and no new peaks were observed. The above information suggested that after the second run, ZIF-67 was transformed to amorphous powder. Thus, the adsorption of Cr(VI) by ZIF-67 could be a self-sacrifice process.

The color of the samples is shown in Fig. 3 and as it is displayed, the color of the samples changed from purple to brown before and after Cr(VI) adsorption for each run. The color change of solid was possibly due to the change of the structure as well as the adsorption of Cr(VI).

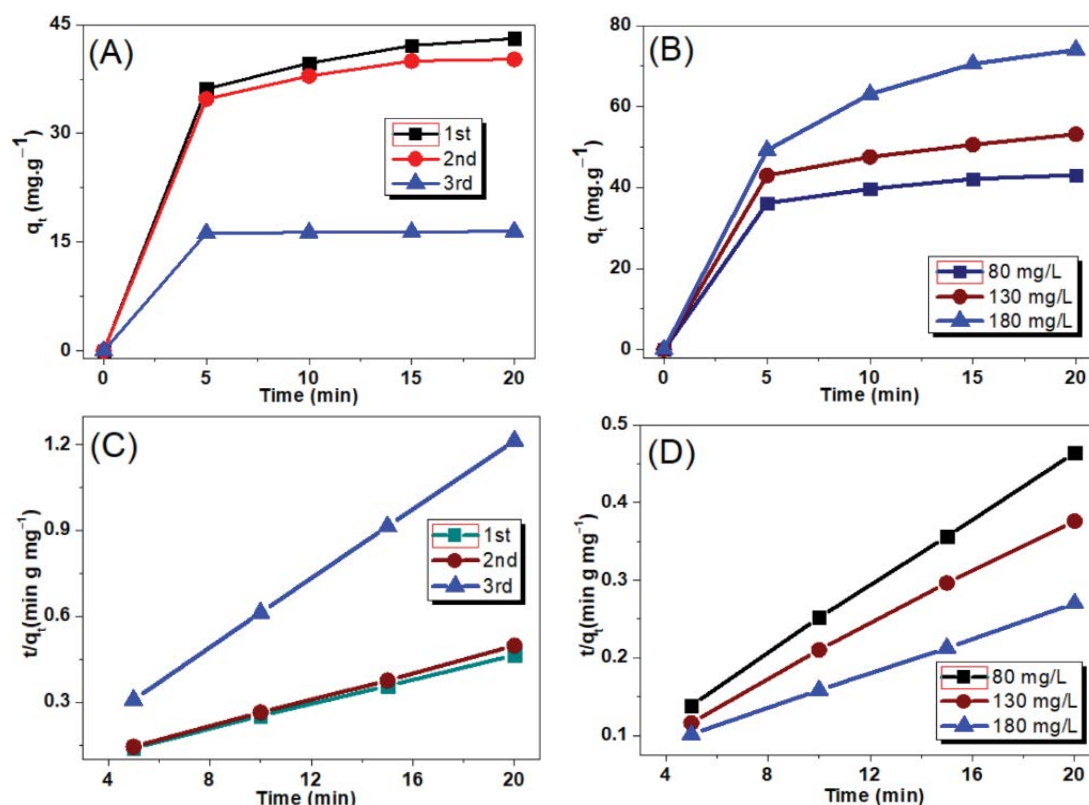


Fig. 1. Change in adsorption capacity of ZIF-67 for three different runs (A), at different Cr(VI) concentration (B), pseudo-second-order kinetic plots of Cr(VI) adsorption for different runs (C) and different Cr(VI) concentration (D).

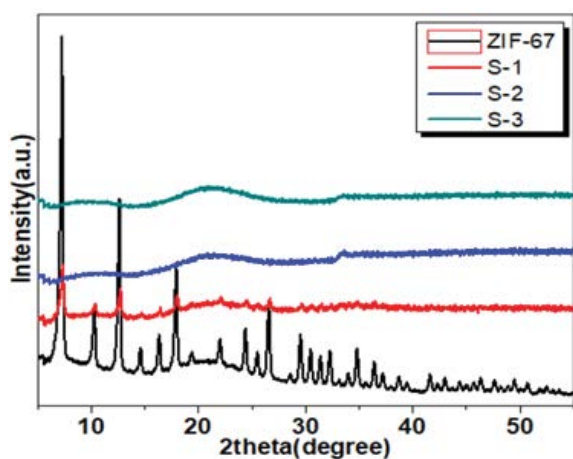


Fig. 2. XRD patterns of fresh ZIF-67 and used for first, second as well as third run of Cr(VI) adsorption.

Thus, the morphology of ZIF-67 at different stages was investigated by FE-SEM.

As shown in Fig. 4, the FE-SEM image of fresh ZIF-67 indicated a structure of polyhedron. After the first run of Cr(VI) adsorption, it was obvious that the polyhedron was broken and the sheet shaped species was obvious. Notably, for the second and third run, the polyhedron was disappeared. Taking into account of the high oxidation ability of Cr(VI), it was suggested that the significant structure



Fig. 3. Photos of the fresh ZIF-67 and after Cr(VI) adsorption for each run.

change was derived from the oxidation–reduction process as well as the variation of pH from 8 to 10.

In order to evidence the change of the chemical state, XPS analysis was performed for the S-3. As shown in Fig. 5A for the Co2p, two main peaks with the binding energy of 796.6 and 780.1 eV were due to the Co2p 1/2 and Co 2p 3/2, respectively [11]. Although it was difficult to judge the oxidation state of cobalt, it was indicated that the binding energy gap between Co 2p main and satellite peak could be a useful standard and the 5.4 eV of the energy gap confirmed the main existence of Co(II) in the S-3 [12]. The results suggested that Co(II) was not oxidized by Cr(VI) during the adsorption.

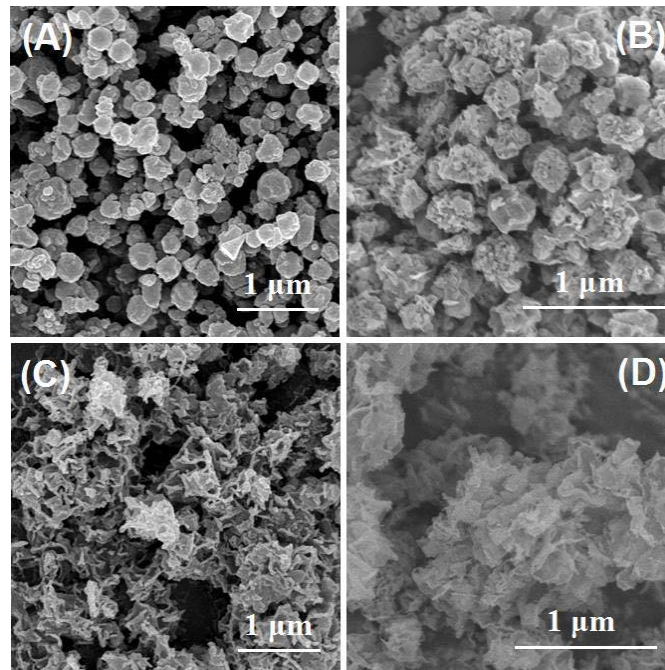


Fig. 4. SEM images of fresh ZIF-67 (A) and after first (B), second (C) as well as third (D) adsorption run.

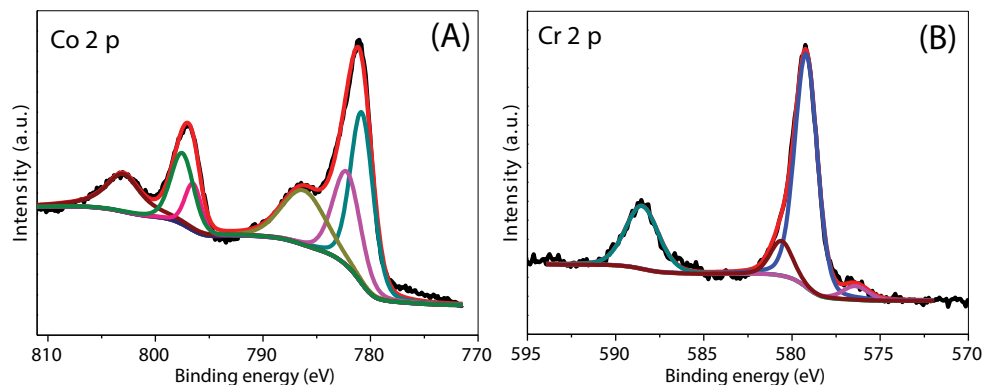


Fig. 5. XPS spectra of Co 2p (A) and Cr 2p (B).

On the other hand, for Cr 2p XPS spectrum, the Cr (2p_{3/2}) peaks located at binding energy 579.2 and 580.6 eV as well as 588.5 eV (Cr 2p_{1/2}) could be contributed to Cr(VI) and in addition, the tiny peak located at 576.3 eV could be due to the Cr(III) species [13,14]. Thus, it seemed that the Cr(VI) species were main ions located at the S-3 and a reduction process could be confirmed.

Based on the above structure analysis and the proposed mechanism in the previous work [15], first of all, the initial Cr(VI) ion concentration gradient and electrostatic interactions led to an efficient mass transfer of Cr(VI) from the bulk solution to the surfaces of the ZIF-67 nanocrystals and then, the uncoordinated Co(II) in surface terminated ZIF-67 nanocrystal served as the active sites of adsorption of Cr(VI). During this process, a partial reduction of the adsorbed Cr(VI) to Cr(III) by electron donated framework on the surface of the ZIF-67 occurred and resulted in the structure damage.

5. Conclusion

A ZIF-67 nanocrystal was synthesized by a facile hydrothermal method with assistance of ammonia and used for the adsorption removal of Cr(VI) with relatively higher concentrations. It was found that the ZIF-67 nanocrystal could be reused for twice with a Langmuir model and the reduction of Cr(VI) and pH variation was observed during the adsorption. A great change of the color of ZIF-67 was found and the structure as well as composition analysis from XRD, XPS as well as FE-SEM suggested that the significant change of the composition and structure of the ZIF-67 was occurred. The reconsideration of ZIF-67 for the adsorption of Cr(VI) with strong oxidability should be noticed.

Declaration of interest statement

The author declares no competing financial interest.

Acknowledgment

This work is supported by University Synergy Innovation Program (GXXT-2019-019) and the Domestic Visiting Scholar Program for Outstanding Young Talents of Anhui Province (No. xgnfx2021135).

References

- [1] N. Liu, M. Tang, C. Jing, W.Y. Huang, P. Tao, X.D. Zhang, J.Q. Lei, L. Tang, Synthesis of highly efficient Co_3O_4 catalysts by heat treatment ZIF-67 for CO oxidation, *J. Sol-Gel Sci. Technol.*, 88 (2018) 163–171.
- [2] G.H. Zhong, D.X. Liu, J.Y. Zhang, The application of ZIF-67 and its derivatives: adsorption, separation, electrochemistry and catalysts, *J. Mater. Chem. A*, 6 (2018) 1887–1899.
- [3] K.Y.A. Lin, H.A. Chang, Ultra-high adsorption capacity of zeolitic imidazole framework-67 (ZIF-67) for removal of malachite green from water, *Chemosphere*, 139 (2015) 624–631.
- [4] S. Saghir, Z.G. Xiao, Synthesis of novel $\text{Ag}@$ ZIF-67 rhombic dodecahedron for enhanced adsorptive removal of antibiotic and organic dye, *J. Mol. Liq.*, 328 (2021) 115323, doi: 10.1016/j.molliq.2021.115323.
- [5] W. Liu, L.D. Jin, J. Xu, J. Liu, Y.Y. Li, P.P. Zhou, C.C. Wang, R.A. Dahlgren, X.D. Wang, Insight into pH dependent Cr(VI) removal with magnetic Fe_3S_4 , *Chem. Eng. J.*, 359 (2019) 564–571.
- [6] J. Shang, Y.N. Guo, D.L. He, W. Qu, Y.N. Tang, L. Zhou, R.L. Zhu, A novel graphene oxide-dicationic ionic liquid composite for Cr(VI) adsorption from aqueous solutions, *J. Hazard. Mater.*, 416 (2021) 125706, doi: 10.1016/j.jhazmat.2021.125706.
- [7] H. Karimi-Maleh, Y. Orooji, A. Ayati, S. Qanbari, B. Tanhaei, F. Karimi, M. Alizadeh, J. Rouhi, L. Fu, M. Sillanpää, Recent advances in removal techniques of Cr(VI) toxic ion from aqueous solution: a comprehensive review, *J. Mol. Liq.*, 329 (2021) 115062, doi: 10.1016/j.molliq.2020.115062.
- [8] A.M. Omer, M.A. El-Monaem, M.M.A. El-Latif, G.M. El-Subruiti, S. Eltaweil, Facile fabrication of novel magnetic ZIF-67 MOF@aminated chitosan composite beads for the adsorptive removal of Cr(VI) from aqueous solutions, *Carbohydr. Polym.*, 265 (2021) 118084, doi: 10.1016/j.carbpol.2021.118084.
- [9] H.J. Hu, J.Y. Liu, Z.H. Xu, L.Y. Zhang, B. Cheng, W.K. Ho, Hierarchical porous Ni/Co-LDH hollow dodecahedron with excellent adsorption property for Congo red and Cr(VI) ions, *Appl. Surf. Sci.*, 478 (2019) 981–990.
- [10] L. Bai, J.X. He, L. Liu, Z.Y. Guan, G.L. Wang, Tunable synthesis of cage-like $\text{Co}_3\text{O}_4/\text{N-C}$ composite and nest-like Co_3O_4 for oxidative degradation of Bisphenol A, *J. Solid State Chem.*, 304 (2021) 122550, doi: 10.1016/j.jssc.2021.122550.
- [11] L. Bai, J.R. Zhang, J.X. He, H.X. Zheng, Q.Y. Yang, ZnO- $\text{Co}_3\text{O}_4/\text{N-C}$ cage derived from hollow Zn/Co ZIF for enhanced degradation of Bisphenol A with persulfate, *Inorg. Chem.*, 60 (2021) 13041–13050.
- [12] J.N. Qin, S.B. Wang, X.C. Wang, Visible-light reduction CO_2 with dodecahedral zeolitic imidazolate framework ZIF-67 as an efficient co-catalyst, *Appl. Catal., B*, 209 (2017) 476–482.
- [13] A.B. Gaspar, C.A.C. Perez, L.C. Dieguez, Characterization of Cr/SiO₂ catalysts and ethylene polymerization by XPS, *Appl. Surf. Sci.*, 252 (2005) 939–949.
- [14] B.A. Manning, J.R. Kiser, H. Kwon, S.R. Kanel, Spectroscopic investigation of Cr(III)- and Cr(VI)-treated nanoscale zerovalent iron, *Environ. Sci. Technol.*, 41 (2007) 586–592.
- [15] X.Y. Li, X.Y. Gao, L.H. Ai, J. Jiang, Mechanistic insight into the interaction and adsorption of Cr(VI) with zeolitic imidazolate framework-67 microcrystals from aqueous solution, *Chem. Eng. J.*, 274 (2015) 238–246.

Supporting information

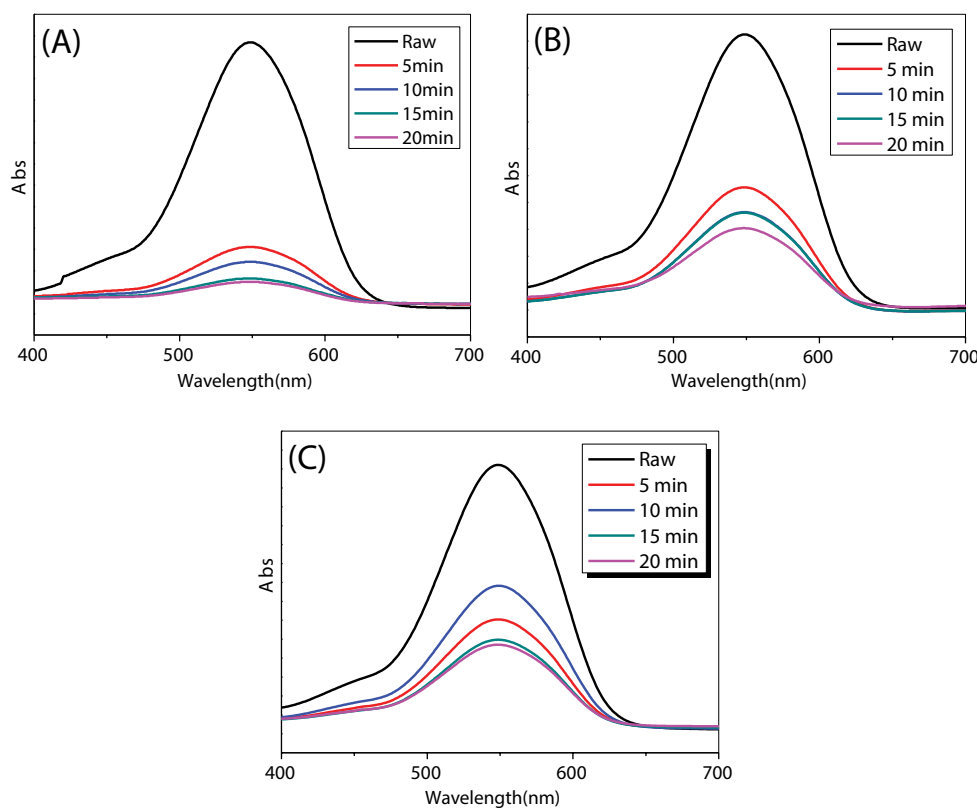


Fig. S1. UV-Vis spectra of Cr(VI) at different time: (A) 80 mg/L, (B) 130 mg/L and (C) 180 mg/L.

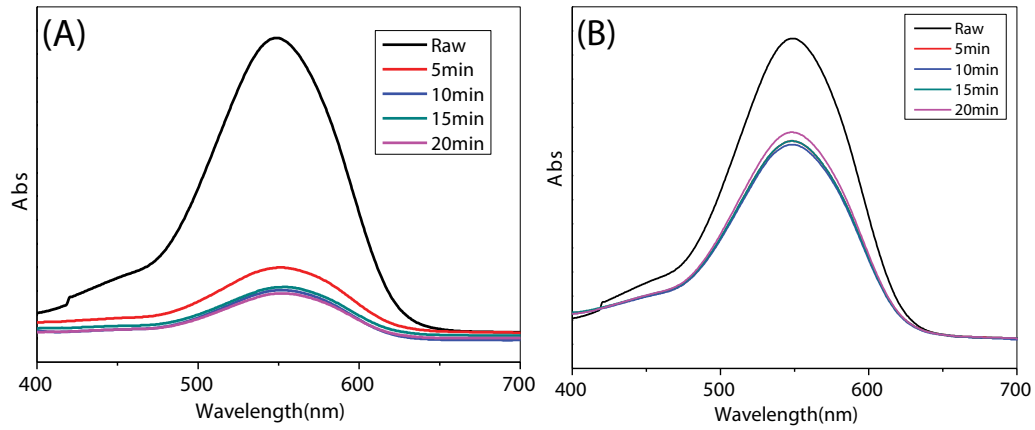


Fig. S2. UV-Vis spectra of Cr(VI) after adsorption over ZIF-67 for second (A) and third run (B).

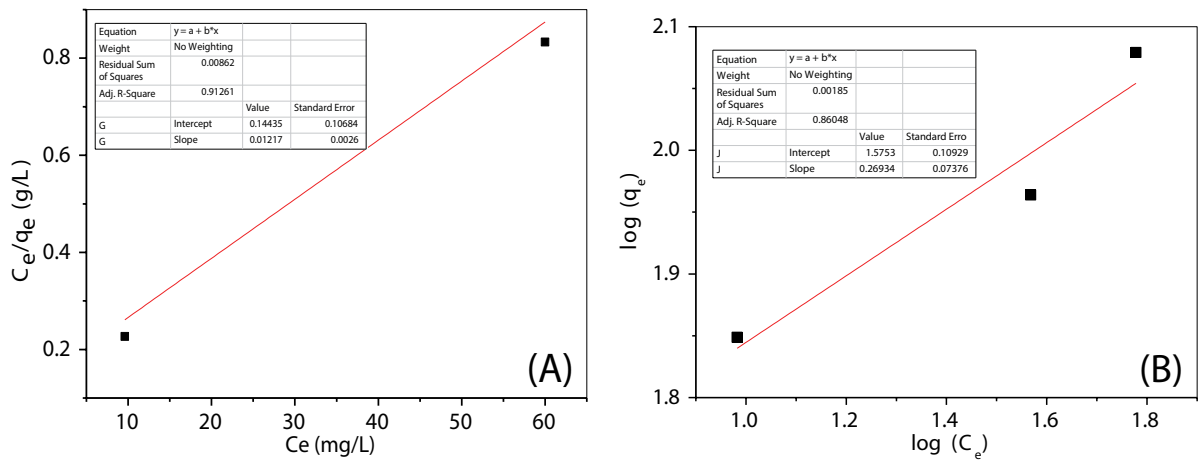


Fig. S3. Langmuir (A) and Freundlich (B) linear plots for the adsorption of Cr(VI).